

EFFECT OF ELECTRON STRUCTURE ON THE COMPRESSIBILITY OF METALS AT HIGH PRESSURE

L. V. AL'TSHULER, A. A. BAKANOVA, and I. P. DUDOLADOV

Submitted July 15, 1967

Zh. Eksp. Teor. Fiz. 53, 1967-1977 (December, 1967)

The shock-wave and shock-compressibility curve parameters are determined for four alkali earth, eight rare earth and five transition metals of groups IV and V of the periodic table at pressures up to 1-4 Mbar. In all the elements measured, except Mg, a strong discontinuous increase in the slopes of the shock adiabat has been observed. The kinks on the compression curves are confirmed by measurements of the isentropic compressibility of Ca. The sharp increase in the elasticity of the metals studied is considered by the authors as the result of electron transitions that lead to the formation of weakly compressible electron configurations. Weakly compressible states due to compression are observed in metals of the last two groups of the periodic table, which are located on descending branches of the atomic volume curve, that is, in elements in which an increase in the number of d electrons leads to an increase in the cohesive forces and the density.

THE realignment of the electronic structure of metals, brought about by compression, takes place without change in the symmetry and type of crystal lattice and also has all the marks of a phase transition. At low temperatures, the electron transitions represent first-order phase transitions, and at higher temperatures, of second order.^[1] The viewpoint developed in^[1] is confirmed by the behavior of Ce^[2,3], which has two isomorphous phases, which differ only in density and the number of valence electrons. The line of phase equilibrium separating them is terminated at 18 kbar by the critical point, above which strong discontinuities are not recorded on the dilatometric curves and the curves of electrical resistance.

In addition to Ce, electronic transformations were observed in static experiments in Cs at 45 kbar^[4,5] and with a lesser degree of reliability in Ba^[6] at 140 kbar. The observed contraction in the volume of Ce, Cs, and Ba is explained by the increase in the number of their valence electrons. Similar phenomena can be expected also in many other metals with incomplete d-shells. For experimental proof of this assumption, the authors undertook the study, over a wide range of pressures, of the shock compression curves of the alkali earths (Mg, Ca, Sr, Ba), the rare earths¹⁾ (La, Ce, Nd, Sm, Gd, Dy, Er, Lu) and a number of transition metals of groups IV and V (Sc, V, Y, Zr, Nb).

The results are given in Sec. 1 of the paper along with data on the isentropic compressibility of Ca. Section 2 is devoted to a discussion of the experimental results and their comparison with the previously obtained characteristics of the shock compressibility of metals with a different electronic structure.

1. METHOD OF INVESTIGATION AND EXPERIMENTAL RESULTS

To obtain high pressures, the authors used explosion setups^[9,10] which produce shock waves of various in-

tensities in screens that cover the specimens. One of them, with a typical location of the specimens, is shown schematically in Fig. 1. In calibration experiments, the velocities of the shock waves were measured by electrical contact pickups in standard samples prepared of the same materials as the screens. The latter were made of copper, aluminum and iron, that is, of metals with well-known dynamic adiabats. In the D-U coordinates, these adiabats are described by the relations^[9,11]

$$\begin{aligned} D(\text{Cu}) &= 3.95 + 1.50U & (0 < U < 4.0), \\ D(\text{Al}) &= 5.25 + 1.39U & (0 < U < 6.0), \\ D(\text{Fe}) &= 3.85 + 1.615U & (1 < U < 4.6), \end{aligned} \quad (1)$$

(the values of D and U are in km/sec), which allow the calculation of the mass velocity U, the pressure $P = \rho_0 DU$ (conservation of momentum) and density $\rho = \rho_0 D (D - U)^{-1}$ (conservation of mass) from the wave velocity U. The results of the determination of the parameters of a number of explosion setups, on which most of the measurements were made, are given in Table I.

On the basis of a series of experiments, the wave velocities were found from measurements with samples of the metals to be investigated. They were obtained by averaging the results of several identical experiments. The error in the determination of the quantity D_M did not exceed 1%.

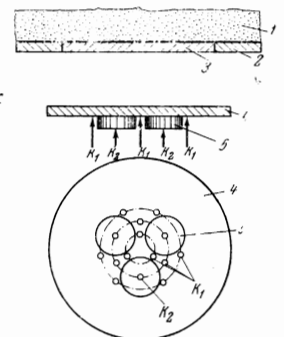


FIG. 1. Experimental arrangement for the measurement of velocities of shock waves with amplitude 600-900 kbar: 1—explosive charge, 2—steel yoke, 3—aluminum striker, 4—aluminum screen, 5—samples under study, K_1 , K_2 —upper and lower contacts.

¹⁾Preliminary data for a number of rare earths and alkali earth metals were briefly reported in [7,8].

Table I.

No. of explosion setup	Screen material ρ_0 , g/cm ³	Shock wave parameters in calibrated specimens			
		U, km/sec	D, km/sec	P, kbar	σ
1	Al; 2.71	0.69	6.21	116	1.126
2	Al; 2.71	1.50	7.34	298	1.258
3	Cu; 8.93	1.67	6.45	961	1.350
4	Al; 2.71	2.82	9.17	700	1.445
5	Fe; 7.85	3.08	8.83	2140	1.536
6	Fe; 7.85	4.56	11.21	4010	1.685

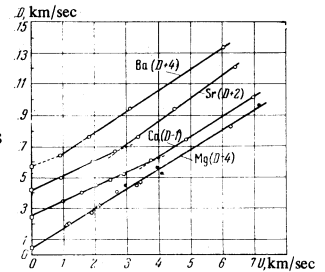
As in [12,13], the initial states of shock compression were revealed on the P-U diagram by the intersection of the "wave rays" $P = \rho_0 M_{DM} U$ with the isentropes of the expansion of the screens. The latter were al-

Table II.

Explosion setup	Shock wave parameters in investigated metals				Explosion setup	Shock wave parameters in investigated metals			
	D, km/sec	U, km/sec	P, kbar	σ		D, km/sec	U, km/sec	P, kbar	σ
La (HCP), $\rho_0 = 6.15$, $C_0 = 2.22$									
—	2.34	0.24	34	1.114	—	7.08	2.08	256	1.416
—	2.67	0.48	79	1.219	—	8.02	2.67	372	1.499
1	2.79	0.68	117	1.322	—	8.49	3.30	487	1.636
—	3.26	1.10	221	1.509	4	8.63	3.39	509	1.647
2	3.70	1.41	321	1.616	—	12.24	6.25	1330	2.043
—	4.03	1.66	417	1.686	—	—	—	—	—
4	5.35	2.49	820	1.871	1	4.43	0.96	64.6	1.277
5	6.95	3.65	1560	2.106	—	4.96	1.59	120	1.472
6	9.09	5.27	2946	2.380	2	5.48	2.04	170	1.593
Zr (FCC), $\rho_0 = 6.75$, $C_0 = 1.71$									
—	2.10	0.0	70.8	1.313	—	5.78	2.46	216	1.741
1	2.37	0.71	113.6	1.428	—	6.18	2.89	271	1.878
2	3.56	1.38	332	1.633	4	7.02	3.77	402	2.160
4	5.17	2.42	845	1.880	5	8.42	4.84	619	2.352
5	6.93	3.54	1656	2.044	6	11.13	6.96	1178	2.670
6	9.08	5.12	3133	2.293	—	—	—	—	—
Nd (HCP), $\rho_0 = 7.0$, $C_0 = 2.15$									
1	2.75	0.66	127	1.316	—	2.93	0.93	70.8	1.465
2	3.48	1.38	336	1.657	1	3.94	1.92	196.7	1.950
4	4.76	2.48	826	2.088	2	4.64	2.63	317	2.308
5	6.62	3.54	1640	2.149	3	5.55	3.35	483	2.523
6	8.88	5.09	3164	2.343	4	7.37	4.49	860	2.559
Sm (R), $\rho_0 = 7.50$, $C_0 = 2.26$									
1	2.71	0.63	128	1.303	5	10.08	6.40	1677	2.739
2	3.42	1.34	344	1.644	—	—	—	—	—
3	4.28	2.09	671	1.954	1	2.34	0.90	76.4	1.625
4	4.65	2.43	847	2.095	2	3.56	1.79	231	2.011
5	6.49	3.49	1699	2.163	4	5.37	3.11	606	2.376
6	8.78	5.00	3293	2.323	6	9.36	6.03	2049	2.811
Gd (HCP), $\rho_0 = 7.93$, $C_0 = 2.25$									
1	2.83	0.60	135	1.269	—	—	—	—	—
2	3.51	1.28	356	1.574	1	5.63	0.69	120	1.140
4	4.79	2.33	885	1.947	2	6.09	1.56	294	1.344
5	6.26	3.48	1728	2.252	4	7.31	2.93	662	1.669
6	8.29	5.00	3287	2.520	5	8.42	4.16	1082	1.977
Dy (HCP), $\rho_0 = 8.52$, $C_0 = 2.19$									
1	2.85	0.57	138.4	1.250	6	10.94	6.04	2042	2.233
2	3.38	1.26	362.8	1.594	—	—	—	—	—
—	3.57	1.47	447	1.700	1	5.86	0.46	164	1.085
3	4.23	1.99	717	1.888	2	6.42	1.08	422	1.202
4	4.56	2.30	893	2.018	4	7.53	2.12	970	1.392
5	6.20	3.4	1796	2.214	5	8.94	3.37	1832	1.605
6	8.22	4.89	3425	2.468	6	11.33	4.92	3389	1.768
Er (HCP), $\rho_0 = 9.05$, $C_0 = 2.26$									
1	2.84	0.56	144	1.246	—	—	—	—	—
2	3.44	1.21	377	1.543	1	3.85	0.69	119	1.218
3	4.20	1.96	745	1.875	2	4.46	1.52	304	1.517
4	4.56	2.23	920	1.957	—	5.36	2.37	570	1.793
5	6.01	3.37	1833	2.277	4	5.82	2.77	724	1.908
6	8.22	4.79	3563	2.397	—	5.79	2.71	705	1.880
Lu (HCP), $\rho_0 = 9.74$, $C_0 = 2.13$									
1	2.76	0.54	145	1.243	5	7.45	3.92	1311	2.110
2	3.38	1.17	385	1.529	6	10.13	5.59	2542	2.230
4	4.53	2.16	953	1.911	—	—	—	—	—
6	8.56	4.60	3835	2.162	1	4.28	0.54	150	1.144
Mg (HCP), $\rho_0 = 1.74$, $C_0 = 4.39$									
—	5.99	1.12	116.7	1.230	2	4.78	1.22	380	1.343
2	6.65	1.85	214.4	1.385	—	5.77	2.08	782	1.564
—	—	—	—	—	4	6.21	2.26	913	1.572
—	—	—	—	—	5	7.68	3.47	1735	1.824
—	—	—	—	—	6	9.87	5.04	3238	2.043

Note: In the table, the following crystalline designations are listed: HCP—hexagonal close packed; FCC—face-centered cubic; BCC—body-centered cubic; R—rhombohedral. The initial sound velocities C_0 (in km/sec) are data from [14,15] is stated in g/cm³.

FIG. 2. D-U diagrams of alkali-earth metals: ○—experimental points of the authors, Δ—data of Walsh et al. [16], ●—results of Skidmore and Morris, [17] □—initial sound velocities C_0 computed from the coefficients of compressibility, [14,15] dashed lines—extrapolations of portions of the D-U relation.



ways approximated by mirror reflections of the shock adiabats. The validity of the "mirror" approximation for large pressure drops (screen-sample) was confirmed by point-by-point construction of the path of isentropes, computed from the equations of state of Cu, Al, and Fe from [9,11].

The experimental data on the shock compressibility of 17 investigated elements are given in Table II. The results of the investigation are represented in D-U coordinates in Fig. 2-4.

As the presented material shows, for all metals except Ba, Ce, and Mg, the points of the D-U diagram are located on two intersecting sections of different slope. Their analytic description by the linear expressions $D = C_0 + \lambda U$ is given in Table III, where the parameters C_0 and λ in the D-U relations are listed for the left (index 1) and right (index 2) sides of the diagrams. The parameters, by means of equations of the form [18]

$$P = \rho_0 C_0 \frac{(\sigma - 1)\sigma}{(\lambda - 1)^2 [\lambda / (\lambda - 1) - \sigma]^2} \quad (2)$$

determine in Figs. 5-8 the positions of the adiabats in the variables $P - \sigma$ (the degree of compression $\sigma = \rho/\rho_0$).

The increase in the jump of the slope of the straight-line segments of the adiabats testifies to the rapid de-

FIG. 3. D-U diagrams of Sc, V, Y, Zr and Nb. The designations are the same as in Fig. 2; X—data of McQueen and Marsh. [13]

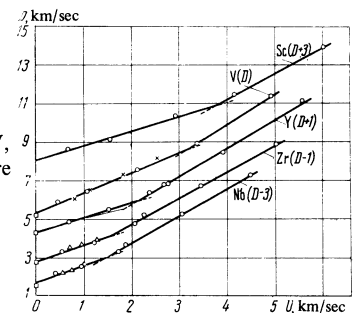


FIG. 4. D-U diagrams of lanthanides. Designations are the same as in Fig. 2.

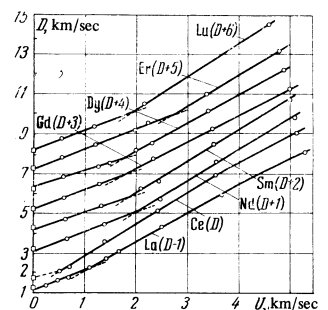


Table III

Metal	C_{01} , km/sec	λ_1	C_{02} , km/sec	λ_2	U_c , km/sec	P_c , kbar	σ_c	$(\frac{dP}{d\sigma})_H^1$, 10^4 kbar	$(\frac{dP}{d\sigma})_H^2$, 10^4 kbar
La*	2.16	1.0	1.65	1.46	1.11	220	1,514	5.6	8.3
Ce*	—	—	1.27	1.596	<0.7	<110	—	—	—
Nd	2.08	1.015	0.90	1.585	2.07	610	1,981	9.5	26.0
Sm	2.19	0.88	0.84	1.600	1.87	540	1,954	7.0	24.0
Gd	2.25	0.98	1.650	1.325	1.74	545	1,785	10.0	15.0
Dy	2.37	0.81	1.34	1.417	1.70	540	1,829	7.8	16.5
Er	2.20	1.033	0.77	1.560	2.71	1230	2,185	16.8	57.0
Lu	2.20	1.00	0.98	1.65	1.88	750	1,854	12.8	31.5
Mg	4.41	1.27	—	—	—	—	—	—	—
Ca	3.55	0.912	2.08	1.308	3.71	390	2,152	4.5	9.0
Sr	2.10	0.94	0.58	1.50	2.71	328	2,400	3.5	15.0
Ba	—	—	1.11	1.365	<0.9	<75	—	—	—
Sc	5.05	0.746	2.83	1.342	3.72	910	1,903	11.0	21.0
V	5.34	1.031	3.74	1.541	3.14	1640	1,577	40.0	64.5
Y	3.33	0.753	1.86	1.455	2.09	460	1,744	7.0	15.0
Zr	3.79	0.877	3.05	1.344	1.58	530	1,440	14.5	20.0
Nb	4.70	0.920	3.91	1.409	1.62	850	1,354	23.0	39.0

*For La and Ce, the description of the right hand (index 2) portions of the D-U diagrams by linear relations are valid for $U \leq 4.0$ km/sec.

crease in the compressibility of metals with increase in pressure. For Ba and Ce, the location of the left-hand portions of the adiabats was not made clear in the experiments of the authors. However, for Ba and for Ce, extrapolation of the right-hand parts of the D-U diagrams to zero pressure does not lead to correct values of the sound velocities under normal conditions. Evidently, singularities in the shock adiabats take place also for these elements, but at much lower pressures, not studied in the dynamic experiments. No singularities and breaks were discovered in the shock adiabats of Mg.

The characteristics of the kinks in the adiabats were found from the intersection of the left and right sides of the lines of the D-U diagrams. The results of these determinations are given on the right-hand side of Table II. The two values of the slopes of the adiabats $(\frac{dP}{d\sigma})_H$ at the critical points are also given there. The slopes were computed from the easily derived relation

$$\left(\frac{dP}{d\sigma}\right)_H = \rho_0 \frac{(D_c + \lambda U_c)(D_c - U_c)^2}{C_0} \quad (3)$$

Because of the possible variations in the choice of the constants C_{01} , λ_1 , C_{02} , and λ_2 , the parameters of the critical points are not uniquely determined. In most cases, the uncertainty in U_c is equal to ± 200 m/sec.

Additional information on the detailed course of the compression curves in the critical region for Ca is obtained from measurements of the sound velocity by means of the relation $C^2 = (\partial P / \partial \rho)_S$, which determines the slope of the isentropes. The method of recording the sound pulses, developed in [19], is based on the appearance of the damping curves of the shock waves created in the medium under study by a blow on the thin plates. A schematically possible picture of the motion of the shock waves and the expansion waves in the case in which there are breaks on the isentropes is sketched on the path-time diagram (Fig. 9). For a smooth form of the isentropes, behind the region of constant flow ABD there is a central relaxation wave which produces a monotonic damping of the sound wave. The presence of a kink on the isentrope means the existence at the critical point of two sound velocities C_1 and C_2 , which differ by a finite amount. As a consequence of this, a second region of constant current (CEF) appears, which is bounded by a segment of the shock wave and the two characteristics $\alpha_1 = C_1 + U_c$ and $\alpha_2 = C_2 + U_c$. The damping curves in this case must have a step shape, with two horizontal portions of constant amplitude.

In the first series of experiments, a 1.5 mm steel plate was used, traveling with a velocity of 5600 m/sec and producing a pressure of 515 kbar in a calcium partition (point I on Fig. 5); this pressure exceeds the critical value by 125 kbar. From constructional considerations, the calcium partitions were covered by a steel screen of the same thickness as the striking

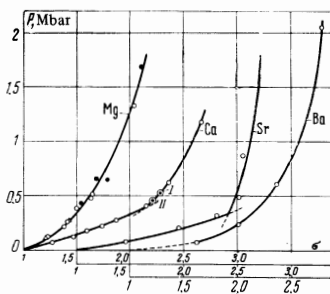


FIG. 5. Shock adiabats of Mg, Ca, Sr and Ba. Designations are the same as in Fig. 2; I, II—initial states in Ca for experiments on damping.

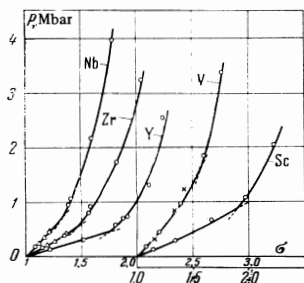


FIG. 6. Shock adiabats of Sc, V, Y, Zr and Nb. Designations are the same as in Fig. 3.

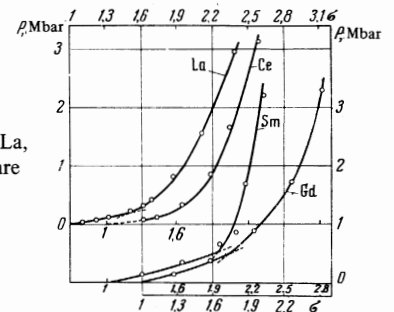


FIG. 7. Shock adiabats of La, Ce, Sm and Gd. Designations are the same as in Fig. 2.

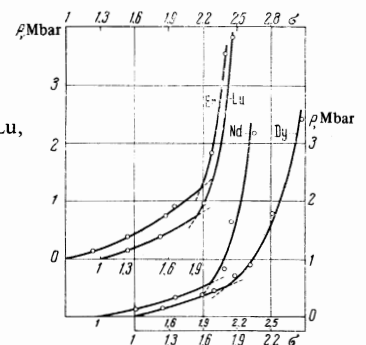


FIG. 8. Shock adiabats of Er, Lu, Nd and Dy. Designations are the same as in Fig. 2.

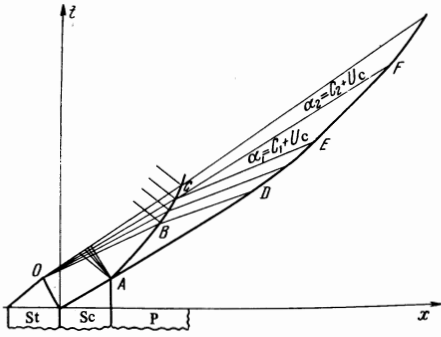


FIG. 9. Scheme for damping of the shock wave in calcium in the presence of breaks on the expansion curves: St—striker plate, Sc—screen, P—Ca partition, O—terminus of the central refraction wave, ABC—trajectory of the screen-specimen boundary, CEF—second region of constant current, AD and EF—portions of trajectory of shock wave with constant amplitude.

plate. The amplitudes of the shock wave for different points of its trajectory were found from the velocities W of motion of the free surface of the calcium partition. The thicknesses of the partitions varied in the range 2 to 22 mm. For each thickness, measurements were carried out in 2–4 identical experiments, which determined the values of W with an accuracy of $\pm \pm 7.0$ m/sec. In a similar apparatus (pressure 450 kbar) another damping curve was obtained for an initial state located on the dynamic adiabat close to the position of the kink (point II in Fig. 5).

The results of all the measurements are shown in Fig. 10 as a function of the path traveled by the wave. Both these curves contain regions of constant amplitude, indicating the presence of break points on the Ca isentropes. The pressures for which breaks appear on the isentropes, below the critical pressure of the discontinuity of the dynamic adiabat (390 kbar), are different for different isentropes. According to the estimates, for expansion from the upper state I (Fig. 5), the break sets in at 290 kbar ($\sigma \approx 1.85$), and for expansion from the lower state (II)—at 200 kb ($\sigma \approx 1.60$). The location of the break points indicates a strong hysteresis which takes place in the return of the Ca to the initial, more compressed state. At other temperatures and pressures and on a different time scale, the same hysteresis phenomenon was discovered for Ce.^[20]

2. DISCUSSION OF THE RESULTS

The discontinuous growth of the derivatives $P_H'(\sigma)$ of the shock adiabats reflects the change in the elasticity of the metals and, in particular, their isentropic elasticity. The connection between the derivatives $P_H'(\sigma)$ and $P_S'(\sigma)$ at the points of inter-

section of the curves $P_H(\sigma)$ and $P_S(\sigma)$ is given by the equation

$$(h - \sigma)P_H = (h - 1)P_S'(\sigma) - P_H\sigma^{-1}, \quad (4)$$

and was first introduced in^[21] in a somewhat different form. The parameter $h = 1 + 2/\gamma$ entering into (4) is expressed in terms of the nondimensional coefficient γ which determines the ratio of the thermal pressure to the volume concentration of thermal energy.

From Eq. (4), for identical on both sides of the kink (the opposite assumption involves the appearance on the adiabats of strong discontinuities which are not observed experimentally), we get the relation

$$\Delta P_S' = \frac{h - \sigma_c}{h - 1} \Delta P_H', \quad (5)$$

which connects the amplitude of the discontinuities of the derivatives of the isentropes and the dynamic adiabats for the critical states.

For the metals under study, according to the estimate, $P_S \approx (0.6-0.8) \Delta P_H'(\sigma)$. The jumps $\Delta P_H'$ are always different in absolute value and, as Table II shows, differ from one another by more than an order of magnitude.

The observed stepwise increase in the elasticity is undoubtedly connected with electron transitions brought about in compressed metals by the deformations of their energy spectra. This point of view is based on the following considerations.

1. In the initial state, most of the metals with kinks on their adiabats have atomic structures which represent different variants of most dense packing (see Table II). It is therefore impossible to explain the decrease in compressibility crystallographically, as the result of a transition to a more dense atomic configuration.

2. Kinks in the compression curves are observed only for those elements where, as the result of the atoms coming closer together, an increase occurs in the number of coupling d-electrons. From this position, the gentle slopes of the initial parts of the adiabats are explained not only by the strong compressibility of the inner s-electrons of the shells, but also by the continuous increase in the number of d-electrons that are free to form strong covalent bonds. The appearance of break points is connected with the completion, at definite degrees of compression, of the process of migration of the electrons and the formation of weakly compressible electron configurations.

Returning to a concrete consideration of these results, we first take up the alkali earth metals. In Mg, which has a normal sequence in the arrangement of the electrons, the metallic properties^[22] are determined by the overlapping of the 3d band and the band of hybrid s-p states. So far as the 3d band is concerned, it is located above the Fermi surface it is not filled in the compression process. This explains the smooth Mg adiabat.

Perfectly clear transitions to the weakly compressible state were established for Ca and Sr at pressures of 390 and 330 kbar, respectively and for a density increase by 2.5 and 2.41 times. According to the classification of Dehlinger,^[20] Ca and Sr are transition metals, inasmuch as their metallic proper-

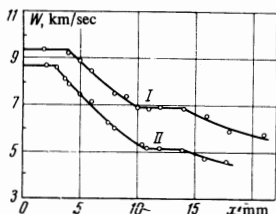


FIG. 10. Damping curves in calcium for two shock wave amplitudes: at 515 kbar (curve I) and 450 kbar (curve II).

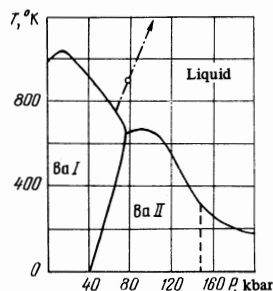


FIG. 11. Phase P-T diagram of Ba according to [3]. Solid curve—melting curve and line of phase equilibrium of Ba I and Ba II; dashed line—line of electron transition according to [3], dot-dash line—initial portion of the experimental shock adiabat, O—point of shock adiabat.

ties arise from the frequency overlapping of their ns bands and their $(n - 1)d$ energy bands (n is the number of the period). Compression of metals leads to the broadening of the energy bands and to a change in their mutual positions—their position approaches the sequence of hydrogenlike atoms. The appearance of singular points in the adiabats and isentropes is naturally explained by completion of the process of transfer of the s electrons to the d level in the critical stages of the compression, when the s band turns out to be located above the Fermi surface.

For Ba, [6] the electronic s-d transitions, which are revealed by jumps in the resistance, occur at pressures of 140 kbar, and are little dependent on the temperature (see Fig. 11). The experimental points of the dynamic measurements, as the P-T diagram shows, lie above its melting curve and characterize the weakly compressible phase. Evidence to this effect is given by the slope of the D-U straight line (Fig. 2) and its extrapolation to zero pressure. The axis of the ordinates of the D-U straight line of Ba intersects at 520 m/sec below its real sound velocity under normal conditions. It is possible that one of the reasons for the change in the compressibility of Ba is the melting process, which increases its density, as is seen from Fig. 11).

The electronic transitions are the only possible reason for the formation of weakly compressible states discovered by the authors in the transition metals of group III—Sc, Y, La and Lu—with the initial electronic structure $ns^2(n - 1)d^1$. The weakest kink in these four metals is observed in La. Among the other transition metals, second-order phase transitions are established in V, Zr, and Nb, but are absent in Mo, Ti [23], W [21] and Cr, and also Fe [11, 18] and Ni [11].

In the aggregate, the results of the present investigation reveal a very clear law—the discontinuous change in the compression always takes place in metals of greater periods, located on the diminishing branches of the curve of atomic volumes $V(Z)$, i.e., for elements for which an increase in the number of d electrons leads to the increase in the force of cohesion and the density. At the present time, only Ti is excluded from this rule [23]. The smooth path of the compression curves is characteristic for the transition metals [11, 21, 23], which are located at the minima of the $V(Z)$ curve, and for close-packed, simple metals. [9, 11, 12] For all these metals, the D-U relations are approximated either by straight lines or by weakly curved lines of diminishing slope.

Among the alkali metals of groups IV–VI, which occupy the maxima of the $V(Z)$ curve, the electronic transitions are established in Cs when it is statically

compressed at 45 kbar; [4] for Rb and K, the possibility of electronic s-d transitions has been shown theoretically, [5, 24] and to a known extent is confirmed by dynamic experiments: for Rb, [25] from the weak kink in its D-U diagram at $U = 2.6$ km/sec ($P = P = 170$ kbar), and for K [26] on the basis of the difference in the thermal pressure of the electrons in the approach to the critical stages of the compression.

The rare earth elements that have been studied are of special importance, especially Ce, Nd, Sm, Gd, Dy, Er, which have partially filled f-levels. In the normal state, these are trivalent metals [2, 27] (electronic formula $4f^{K5d}6s^2$) with different numbers of f-electrons. For Ce, according to [2], the $\gamma - \alpha$ transition at 7 kbar is produced by the excitation of its solitary f-electron and the increase in its valence to 3.67 because of this. No other singularity is observed in the adiabat of Ce up to pressures of 3 Mbar.

The adiabat of Gd has a very weak kink in comparison with the other rare-earth elements; its f-band contains a stable configuration of seven electrons, [27] and also the adiabat of La, which does not generally have f-electrons. The path of the Ce adiabat and the absence in La and Gd of significant changes in the compressibility due to the s-d realignment of the electrons represents a non-trivial difference from Lu and a number of other transition and alkali earth metals. It is very probable, therefore, that in Nd and Sm, which have “unattached” f-electrons and which are located between Ce and Gd, decreasing the compressibility, the electron reorganization is the same as in Ce, which belongs not to the s-d but to the f-d type.

The nature of the electronic redistributions in Dy and Er, which are located in the periodic table between Gd and Lu, is not known at the present time. More definite conclusions on this question can be made after calculation of their energy spectra in the different stages of the compression, for example, according to the method of Gandel'man. [24]

¹R. G. Arkhipov, Zh. Eksp. Teor. Fiz. 49, 1601 (1965) [Sov. Phys. JETP 22, 1095 (1966)].

²I Intern. Conf. in Physics of Solids at High Pressures, Tucson, Arizona, 1965.

³V. V. Evdokimova, Usp. Fiz. Nauk 88, 93 (1966) [Sov. Phys. Usp. 9, 54 (1966)].

⁴P. W. Bridgman, Proc. Amer. Acad. Arts. Sci. 81, 165 (1952).

⁵E. S. Alekseev and R. G. Arkhipov, Fiz. Tverd. Tela 4, 1077 (1962) [Sov. Phys. Solid State 4, 794 (1962)].

⁶H. Drikamer, (Solids under High Pressure (Russ. transl. Mir. 1966).

⁷L. V. Al'tshuler, A. A. Bakanova and I. P. Dudoladov, ZhETF Pis. Red. 3, 483 (1966), [JETP Lett. 3, 315 (1966)].

⁸A. A. Bakanova and I. P. Dudoladov, ZhETF Pis. Red. 5, 322 (1967) [JETP Lett. 5, 265 (1967)].

⁹L. V. Al'tshuler, S. B. Korner, A. A. Bakanova and R. F. Trunin, Zh. Eksp. Teor. Fiz. 38, 790 (1960) [Sov. Phys. JETP 11, 573 (1960)].

¹⁰L. V. Al'tshuler, M. N. Pavlovskii, L. V. Kuleshova and G. V. Simakov, Fiz. Tverd. Tela 5, 279 (1963)

[Sov. Phys. Solid State 5, 203 (1963)].

¹¹L. V. Al'tshuler, A. A. Bakanova and R. F. Trunin, Zh. Eksp. Teor. Fiz. 42, 91 (1962) [Sov. Phys. JETP 15, 65 (1962)].

¹²L. V. Al'tshuler, K. K. Krupnikov and M. I. Brazhnik, Zh. Eksp. Teor. Fiz. 34, 886 (1958) [Sov. Phys. JETP 7, 614 (1958)].

¹³R. G. McQueen and S. P. Marsh, J. Appl. Phys. 31, 1253 (1960).

¹⁴Rare Metals Handbook, Reinhold.

¹⁵C. Kittel, Introduction to Solid State Physics, 3rd Ed., J. Wiley, New York, 1966.

¹⁶J. M. Walsh, M. H. Rice, R. G. McQueen and F. L. Yarger, Phys. Rev. 108, 196 (1957).

¹⁷I. C. Skidmore and E. Morris, Thermodynamics of Nucleus (Proc. of Symposium), Vienna, 1962.

¹⁸L. V. Al'tshuler, K. K. Krupnikov, B. N. Ledenev, V. I. Zhuchikhin and M. I. Brazhnik, Zh. Eksp. Teor. Fiz. 34, 874 (1958) [Sov. Phys. JETP 7, 606 (1958)].

¹⁹L. V. Al'tshuler, S. B. Korner, M. I. Brazhnik, L. A. Vladimirov, M. P. Speranskaya and A. I. Funtikov, Zh. Eksp. Teor. Fiz. 38, 1061 (1960) [Sov. Phys. JETP 11, 766 (1960)].

²⁰V. V. Evdokimova, X-ray studies of certain materials at pressures up to 20 kbar, Dissertation,

Institute of High Pressure Physics, Acad. Sci. USSR, Moscow, 1966.

²¹K. K. Krupnikov, M. I. Brazhnik and V. P. Krupnikova, Zh. Eksp. Teor. Fiz. 42, 675 (1962), [Sov. Phys. JETP 15, 470 (1962)].

²²U. Dehlinger, Theoretical Metal Studies (Russian translation from the German), Gos. nauch, tekhn. izd. lit. po chernoi i tsvetnoi metallurgii, 1960.

²³K. K. Krupnikov, A. A. Bakanova, M. I. Brazhnik and R. F. Tunin, Dokl. Akad. Nauk SSSR 148, 1302 (1963) [Sov. Phys. Dokl. 8, 203 (1963)].

²⁴G. M. Gandel'man, Zh. Eksp. Teor. Fiz. 51, 147 (1966) [Soviet Phys. JETP 24, 99 (1967)].

²⁵M. H. Rice, J. Phys. Chem. Solids 26, 483 (1965).

²⁶A. A. Bakanova, I. P. Dudoladov and R. F. Trunin, Fiz. Tverd. Tela 7, 1615 (1965) [Sov. Phys. Solid State 7, 1307 (1965)].

²⁷E. M. Savitskii, V. F. Terekhov, I. V. Burov, I. A. Markova and O. P. Naumkina, Splavy redkozemel'nykh metallov (Alloys of Rare Earth Metals) (Acad. Sci. USSR Press, 1962).

Translated by R. T. Beyer

224